In Situ Stability of Substrate-Associated Cellulases Studied by DSC

ARTICLE *in* LANGMUIR · JUNE 2014

Impact Factor: 4.46 · DOI: 10.1021/la500161e

8 AUTHORS, INCLUDING:

Kim Borch
Novozymes
40 PUBLICATIONS **663** CITATIONS
SEE PROFILE

Nicolaj Cruys-Bagger
Roskilde University
20 PUBLICATIONS **328** CITATIONS
SEE PROFILE

Silke Badino
Roskilde University
4 PUBLICATIONS **14** CITATIONS
SEE PROFILE

Peter Westh
Roskilde University
183 PUBLICATIONS **3,447** CITATIONS
SEE PROFILE

Langmuir

Article

pubs.acs.org/Langmuir

In Situ Stability of Substrate-Associated Cellulases Studied by DSC

Kadri Alasepp,[†] Kim Borch,[‡] Nicolaj Cruys-Bagger,[†] Silke Badino,[†] Kenneth Jensen,[‡] Trine H. Sørensen,[†] Michael S. Windahl,[†,‡] and Peter Westh*[,†]

[†]Research Unit for Functional Biomaterials, NSM, Roskilde University. 1 Universitetsvej, Build. 18.1, DK-4000 Roskilde Denmark

[‡]Novozymes A/S, Krogshøjvej 36, DK-2880 Bagsværd, Denmark

ABSTRACT: This work shows that differential scanning calorimetry (DSC) can be used to monitor the stability of substrate-adsorbed cellulases during long-term hydrolysis of insoluble cellulose. Thermal transitions of adsorbed enzyme were measured regularly in subsets of a progressing hydrolysis, and the size of the transition peak was used as a gauge of the population of native enzyme. Analogous measurements were made for enzymes in pure buffer. Investigations of two cellobiohydrolases, Cel6A and Cel7A, from *Trichoderma reesei*, which is an anamorph of the fungus *Hypocrea jerorina*, showed that these enzymes were essentially stable at 25 °C. Thus, over a 53 h experiment, Cel6A lost less than 15% of the native population and Cel7A showed no detectable loss for either the free or substrate-adsorbed state. At higher temperatures we found significant losses in the native populations, and at the highest tested temperature (49 °C) about 80% Cel6A and 35% of Cel7A was lost after 53 h of hydrolysis. The data consistently showed that Cel7A was more long-term stable than Cel6A and that substrate-associated enzyme was less long-term stable than enzyme in pure buffer stored under otherwise equal conditions. There was no correlation between the intrinsic stability, specified by the transition temperature in the DSC, and the long-term stability derived from the peak area. The results are discussed with respect to the role of enzyme denaturation for the ubiquitous slowdown observed in the enzymatic hydrolysis of cellulose.

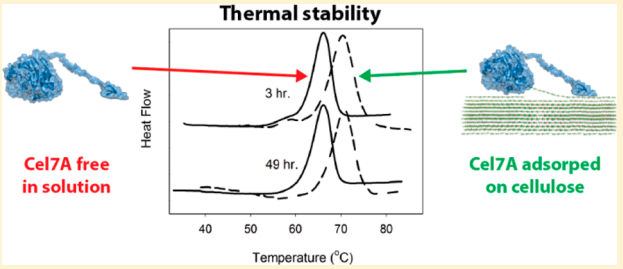

INTRODUCTION

The enzymatic deconstruction of lignocellulosic biomass is a key process for the implementation of sustainable industries based on agricultural residues. This has generated substantial research interest in cellulases, xylanases, lytic monooxygenases, and other enzymes involved in the breakdown of polymers from the plant cell wall.[1−5] Many investigations of these enzymes have found unusual kinetic behavior that could not be readily rationalized by conventional theories. This is at least in part due to the heterogeneous surface of the insoluble substrate and the concomitant diversity of enzyme−substrate complexes, which interconvert on different time scales during the process. One particularly important example of atypical kinetics for cellulolytic enzymes is the ubiquitous slowdown in the hydrolytic activity. Thus, essentially all experimental studies including both monocomponent cellulases and cellulase cocktails and substrates ranging from purified cellulose to complex biomass show a characteristic loss in enzymatic activity as the hydrolysis progresses.[6] This effect can be quite pronounced, and it poses a significant challenge for the industrial application of cellulases as the rate of hydrolysis may fall to exceedingly low levels well before the cellulose is fully converted to soluble sugars. The origins of the slowdown have been discussed extensively, and based on the current understanding it appears reasonable to infer that it relies on several factors. For example, in the later stages of hydrolysis, cellulase activity may be impeded by both accumulated products[7−10] and the depletion of substrate with good reactivity.[11] Another type of rate retardation has been reported in the very early stages, before the reaction reaches quasi-steady state. Thus, cellulases may show a burst (and subsequent slowdown) in activity within seconds or minutes,[12−16] which is akin[17,18] to that found for other hydrolytic enzymes, which cleaves soluble substrates in conventional homogeneous catalysis.[19−21] These factors, however, cannot fully account for the slowdown, which also appears to depend on intricate enzyme−substrate interactions that affect the hydrolytic activity on intermediate and long time scales.[22−24] Recently, our understanding of these interactions has been promoted by studies using surface methods such as QCM, AFM, and SPR.[25−29] Some of these works have visualized the decay of cellulose particles during enzymatic attack, and others have provided quantitative information on the rate and extent of adsorption and hydrolysis. A recurring result in the latter type of work has been a distinct hysteresis (or irreversibility) of the enzyme−cellulose interaction. Thus, only a limited fraction of the adsorbed enzyme can be washed off the substrate in QCM or SPR when the flow above the cellulose surface reverts from an enzyme solution to a pure buffer.[27,29] This notion of irreversible adsorption also occurs in work on suspended cellulose particles, but conclusions in this area remain divisive. The most commonly studied cellulase, Cel7A, for example, has been reported to show no,[30]

Received: January 13, 2014
Revised: May 8, 2014
Published: May 23, 2014

   dx.doi.org/10.1021/la500161e | *Langmuir* 2014, 30, 7134−7142

partial,[31,32] or full[33,34] reversibility when the sample was diluted with buffer. Interestingly, both QCM and SPR showed that the population of enzyme irreversibly bound to cellulose on the measuring chip increased gradually with time,[27,29] and similar behavior, albeit on a much slower time scale, has been found for a bulk suspension of cellulose and Cel7A.[34] This has led to the suggestion that irreversible binding and inactivation may be causally related in the sense that conformational changes of the enzyme underlie both tighter (irreversible) association and inactivation.[29] This latter mechanism is reminiscent of that generally suggested for the irreversible (nonspecific) adsorption of model proteins on different solid sorbents.[35−38] If indeed a population of strongly bound cellulase with non-native conformation tends to build up during hydrolysis, this would clearly have a negative impact on the enzymatic activity and hence would be a contributing factor to the slowdown. This idea is not new, and different types of gradual cellulase inactivation during the hydrolysis have been discussed repeatedly. (See Bansal et al.[6] for a review.) Further insight into this problem appears to rely on better experimental approaches, and in the present work we show that a combination of differential scanning calorimetry (DSC) and standard adsorption and activity measurements may provide quantitative information on the long-term stability of cellulases both free (dissolved in buffer) and in situ during the hydrolysis of insoluble cellulose. We have used this approach in studies of two cellobiohydrolases from *Trichorderma reesei* (an anamorph of the fungus *Hypocrea jecorina*), Cel7A, and Cel6A, which are among the most thoroughly investigated cellulases and candidates for industrial use. Both enzymes consist of a catalytic domain and a carbohydrate binding module (CBM), which are connected by a flexible glycosylated linker. They are thought to hydrolyze cellulose processively, i.e., by sequential catalytic cycles performed on a cellulose strand without dissociation. Cel7A is a retaining enzyme which attacks the reducing end of the cellulase strand, while Cel6A uses the inverting mechanism and starts the processive movement from the nonreducing end.[39] Both enzymes have been reported to hydrolyze microcrystalline cellulose, although recent observations have suggested that Cel6A has a preference for the disordered (noncrystalline) parts[40] of a mixed crystalline/amorphous substrate such as Avicel. (The crystallinity index of Avicel is 0.5−0.7.[41,42]) The maximal enzymatic activity for these enzymes is found at around 55−60 °C,[43,44] and industrial application usually uses temperatures of around 50 °C.

Results of the current work showed that enzyme denaturation may contribute to the slowdown and that the importance of this factor varies strongly with storage temperature and enzyme type.

EXPERIMENTAL SECTION

Materials. Enzymes Cel7A (CBH1) and Cel6A (CBH2) from *Hypocrea jecorina* were cloned, expressed, and purified as described previously.[18,45,46] Enzyme concentrations were derived from measurements of the optical density at 280 nm using theoretical extinction coefficients (86.8 mM^{-1} for Cel7A and 96.6 mM^{-1} for Cel6A) calculated from the amino acid content.[47] All experiments were conducted in a standard 50 mM acetate buffer at pH 5.0. The substrate was Avicel PH101 (Fluka) at an initial load of 60 g/L. Avicel was chosen because it is the most commonly used model substrate, and initial work showed that it was readily handled at high loads and showed no thermal transitions in the DSC.

Procedures. The stability of Cel6A and Cel7A was investigated in thermal stress experiments in which enzyme samples were exposed to a preset storage temperature (T_{store}) for up to 53 h. Cel6A was tested at T_{store} = 25, 40, and 49 °C, and for Cel7A we used T_{store}= 25 and 49 °C. Each thermal stress experiment (i.e., one enzyme studied as a function of time at one value of T_{store}) was started by preparing about 20 aliquots of 1000 μL of enzyme solution in 2 mL Eppendorf tubes. Half of the tubes contained substrate (60 g/L Avicel), while the other half were references, with enzyme dissolved in pure buffer. All samples had an enzyme load of 0.63 mg/mL. Henceforth we will refer to samples with and without Avicel as hydrolysis samples and reference samples, respectively. All samples were placed horizontally in a rack on an orbital shaker in a temperature-controlled incubator and agitated so that the liquid moved gently forth and back in the tube. At given time points, samples were removed from the incubator, degassed under vacuum, and loaded into a differential scanning calorimeter (Nano-DSC, TA Instruments, New Castle, DE) to test the thermal stability. The Nano-DSC was equipped with flow-through capillary cells, which were loaded with pipettes mounted on both the inlet and outlet. This enabled rapid liquid movement forth and back in the capillaries and hence the establishment of a homogeneous suspension of the hydrolysis samples in the cell before the start of the calorimetric experiment (this was essential for the data analysis; see below). The reference cell in the DSC was loaded with pure buffer in all runs. Excess sample from the thermal stress experiments that was not used to load the DSC was saved for other types of analyses described below. The stability of the enzyme was tested in heating scans from 20 to about 85 °C at a rate of 2 °C/min. A distinct thermal transition was evident in all enzyme samples while no transitions could be detected in control experiments with (enzyme-free) Avicel suspension in the calorimeter. We used the Nano-Analyze software package (TA Instruments) to analyze enzyme transitions following the subtraction of either a buffer scan or a scan with a pure Avicel suspension. We did not find systematic differences between T_T and ΔH derived by these two procedures, and this corroborates that the results were unaffected by possible thermal transitions in pure Avicel. The transition temperature was simply defined as the apex of the transition peak, and ΔH was calculated in the conventional way by normalizing the total heat (the area under the transition peak in μJ) with respect to the number of moles of enzyme in the calorimetric cell (299 μL) assuming a homogeneous sample. The total volume required to fill the instrument (~700 μL) includes both the active volume where the heat signal is detected (299 μL) and the volume of the access shaft, which must also be filled with sample (but is not heated during a measurement). Effects of inhomogeneity resulting from the precipitation of Avicel with bound enzyme from the vertical access shaft were taken into account as described in the Results and Data Analysis section. In some cases, the sample was cooled in the instrument after the calorimetric scan was completed, equilibrated at 20 °C for 15 min, and taken through a second heating scan to test if any refolding of the denatured enzyme had occurred.

The remainder of the samples (i.e., the liquid not loaded into the DSC) was centrifuged at 10 000*g* for 3 min. The supernatant was spilt into two and analyzed for the content of soluble sugars (only hydrolysis samples) and the free enzyme (both hydrolysis and reference samples). Free enzyme was quantified by spectrofluorometry using the intrinsic protein fluorescence at an excitation wavelength of 280 nm. The emission at 345 nm was measured in a Shimadzu RF-5301PC instrument and translated into concentration units using standard curves prepared in direct connection to the analysis of the samples. Soluble sugars were quantified in an ICS-5000 ion chromatograph equipped with a CarboPac PA-10 column and an electrochemical detector (Termo Fisher Scientific Waltham, MA). Samples were eluded with a multistep gradient with 50 mM NaOH (0−4 min), 100 mM sodium acetate + 90 mM NaOH (4−28 min), 450 mM sodium acetate + 200 mM NaOH (28−29 min), and 50 mM NaOH (29−35 min). The results were quantified against standards for glucose, cellobiose, and cellotriose run daily.

dx.doi.org/10.1021/la500161e | *Langmuir* 2014, 30, 7134−7142

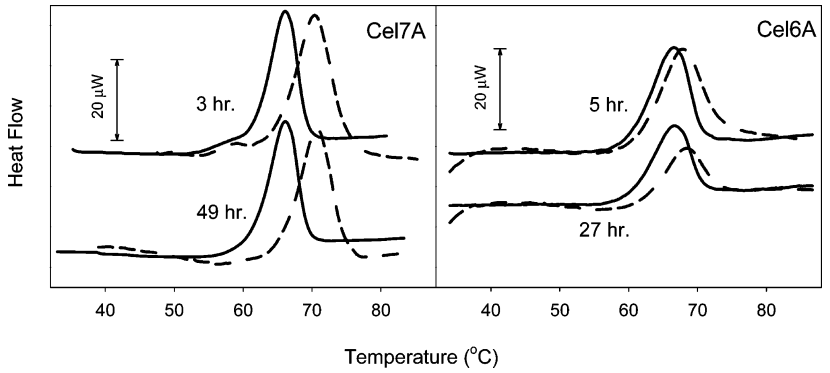

Figure 1. Representative DSC data (so-called thermograms) for Cel7A and Cel6A from thermal stress experiments at T_{store} = 49 °C. Samples were retrieved at the stated time points and analyzed in the DSC. Full lines represent reference samples (0.63 mg/mL of enzyme dissolved in buffer), and dashed curves are hydrolysis samples (0.63 mg/mL of enzyme in a 60 g/L Avicel suspension).

RESULTS AND DATA ANALYSIS

Figure 1 shows representative examples of DSC data (so-called thermograms giving the differential heat flow as a function of temperature). Specifically, thermal transitions of Cel7A and Cel6A are shown for experiments with T_{store} = 49 °C. The samples were retrieved at different time points as stated in the figure. To facilitate comparisons, the thermograms have been shifted vertically so each pair of curves shows a corresponding set of reference (solid line) and hydrolysis (dashed line) samples. For Cel7A, it clearly appears that the presence of substrate displaces the transition temperature, T_T, in an upward direction; the average shift, ΔT, was 4.4 ± 0.3 °C (Table 1).

Table 1. Average Transition Temperatures, T_T, for Enzymes with and without Substrate[a]

enzyme	hydrolysis samples (60 g/L Avicel)	reference samples (buffer)
Cel7A	70.5 ± 0.3 °C (n = 19)	66.1 ± 0.03 °C (n = 18)
Cel6A	66.9 ± 1.3 °C (n = 30)	66.5 ± 0.2 °C (n = 28)

[a] T_T was independent of the storage temperature and duration of the thermal stress experiment prior to the DSC analysis.

For Cel6A a slight shift also appears in the examples in Figure 1, but for this enzyme ΔT was less than the experimental scatter (Table 1). Figure 1 also shows a trend toward smaller peaks (lower ΔH) in samples with long contact times. This is particularly evident for the Cel6A hydrolysis samples, which show a much smaller transition peak after 27 h compared to the 5 h time point. For Cel7A the difference between the two time points is smaller, but the integration of the curves in Figure 1 showed that ΔH had decreased by about 20% between the two time points in the figure (further illustrated in Figures 2 and 3). The calorimetric behavior may be illustrated more clearly by plotting both T_T and ΔH as functions of the contact time. Figure 2 shows examples for Cel7A in thermal stress experiments at 25 and 49 °C, and it appears that T_T was essentially independent of both storage temperature and duration of the thermal stress experiment preceding the DSC measurement. (The T_T lines in Figure 2 are horizontal.) Average values of T_T for both enzymes were therefore calculated for hydrolysis and reference samples and are listed in Table 1.

Figure 2 shows that, depending on the conditions, ΔH may develop very differently over time in thermal stress experiments. For example, ΔH remained constant in reference samples for T_{store} = 25 °C over the entire 53 h experiment but decreased rapidly (particularly during the first 10 h) in hydrolysis samples with T_{store} = 49 °C. Another noticeable

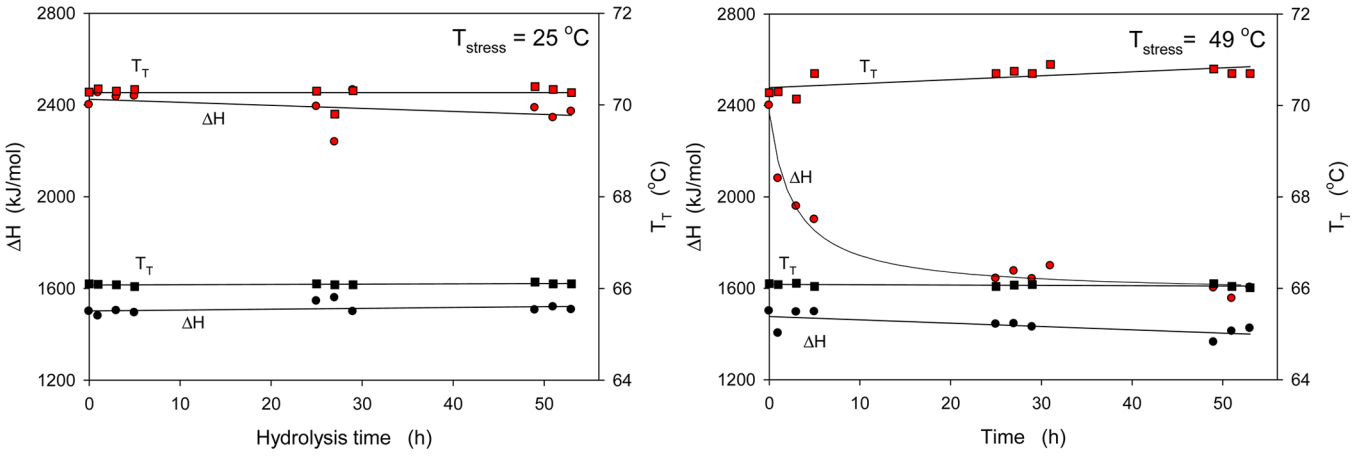

Figure 2. Representative calorimetric data from the thermal stress experiments. The results are for Cel7A at storage temperatures of 25 and 49 °C, and the plots show how the transition temperature, T_T (squares, right ordinate), and the enthalpy change, ΔH (circles, left ordinate), vary with contact time. Red symbols identify hydrolysis samples (with 60 g/L Avicel), and black symbols are reference samples where Cel7A is dissolved in buffer. Overall it appears that T_T is essentially independent of thermal stress and that ΔH decreases at high but not at low storage temperature.

dx.doi.org/10.1021/la500161e | Langmuir 2014, 30, 7134−7142

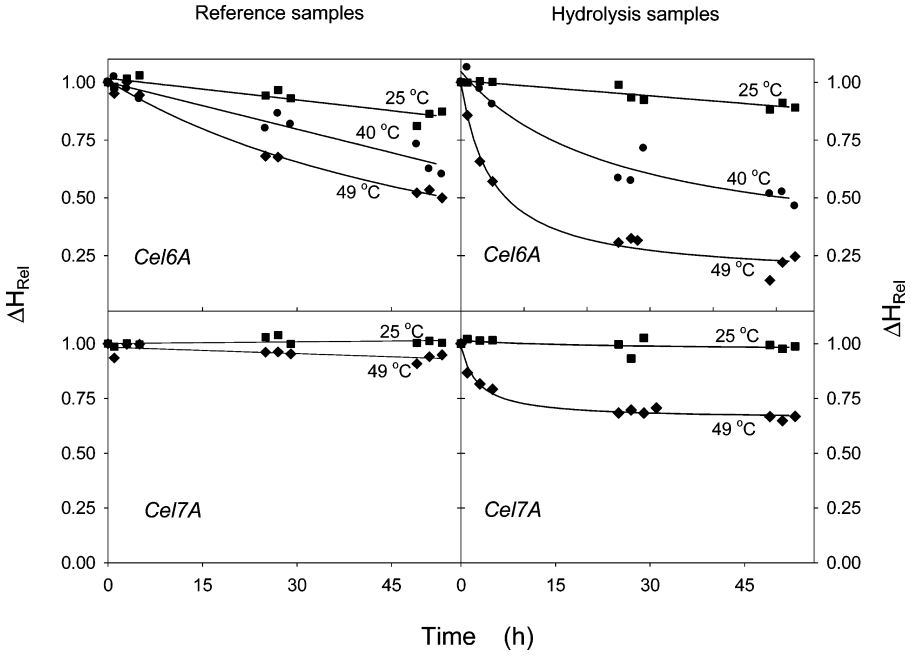

Figure 3. Relative enthalpy changes, $\Delta H_{Rel} = \Delta H/\Delta H_0$, for respectively reference samples (left panels) and hydrolysis samples (right panels) plotted as a function of the duration of thermal stress. (The storage temperature, T_{store}, is identified by the labels.) The fitted curves are without theoretical meaning and are included only to facilitate reading.

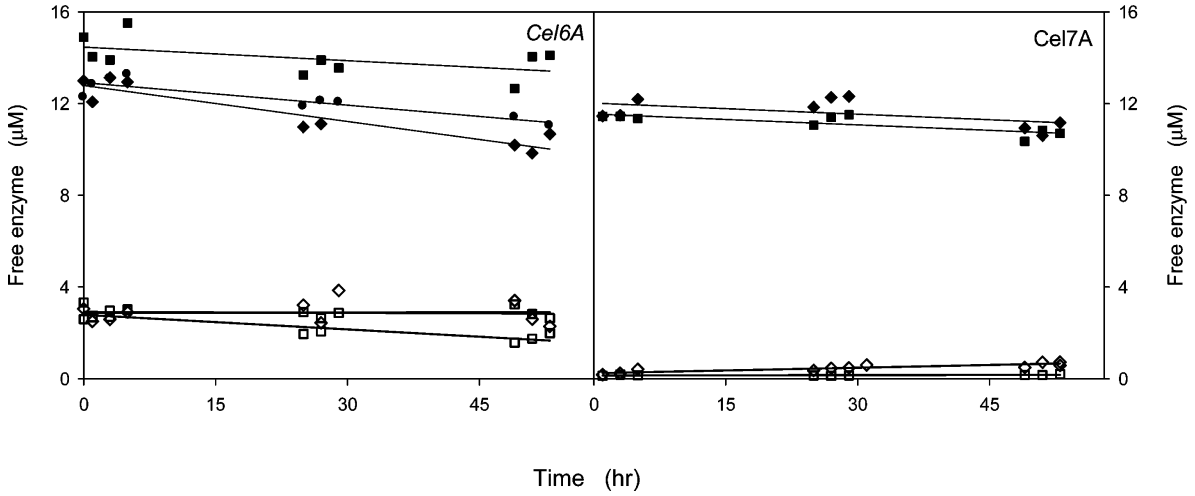

Figure 4. Time dependence of the free (aqueous) enzyme concentration in hydrolysis samples (open symbols) and reference samples (filled symbols). The storage temperatures were 25 °C (squares), 40 °C (circles), and 49 °C (diamonds).

result from Figure 2 was that ΔH was much higher in hydrolysis samples compared to references. This was expected for two reasons. First, protein–ligand interactions tend to increase ΔH due to the extra energy required to break the additional interactions in the complex during the thermal transition.[48] Second, the precipitation of Avicel particles with bound enzyme inevitably increased ΔH for the hydrolysis samples. This follows from the design of the instrument (and indeed all commercial high-sensitivity DSCs) with both the active part of the cell and the vertical access shafts filled with sample. For the hydrolysis samples, Avicel particles with bound enzyme sediment from the access shaft into the active part of the cell during the initial equilibration and hence increase the amount of enzyme there. Obviously, this effect will be absent in the (homogeneous) reference samples. We found that the current protocol (with about 30 min initial equilibration) gave reproducible ΔH and that longer equilibration did not change the observed enthalpy change. Also, a visual inspection of a model of the capillary cell of this instrument made of (transparent) tubing showed that all Avicel had settled within a half hour. On the basis of this we conclude that the absolute ΔH values for the hydrolysis samples (but not the reference samples) in Figure 2 are dependent on the instrument design and hence without direct physical meaning. However, as the change in ΔH is systematic (governed by the volume of the access shaft), the relative changes in ΔH can be used to quantify how the denaturation behavior develops during the course of the thermal stress experiments. We therefore calculated the relative enthalpy change ΔH_{Rel} for all trials by normalizing the value at any given time point with the enthalpy change at time = 0, ΔH_0. The latter was found by extrapolating plots of ΔH vs time to time = 0 (cf. Figure 2). We note that

dx.doi.org/10.1021/la500161e | Langmuir 2014, 30, 7134–7142

ΔH_0 values derived in this way were independent of T_{store}, but as it appears in the example in Figure 2, extrapolations for T_{store} = 25 °C, where the ΔH function was essentially flat, provided the most precise values for ΔH_0. Results in Figure 3 show how ΔH_{Rel} developed with the duration of the thermal stress for all investigated systems.

The Interpretation of the calorimetric data will rely on the populations of free and substrate-associated enzyme in the hydrolysis samples. The results in Figure 4 show that Cel7A is almost fully associated with the substrate under the conditions used here. The free concentrations of this enzyme in the hydrolysis samples were 1−2% (T_{store} = 25 °C) and 2−5% (T_{store} = 49 °C) of the concentration in the references (Figure 4). The interaction of Cel6A and Avicel is weaker, but this enzyme is also predominantly substrate-bound with a free population corresponding to 15−18% of the reference samples. Cel6A showed a decreasing trend in the free concentration, particularly in the reference samples. This is possibly associated with a limited aggregation of enzyme, which is removed in the centrifugation step prior to the fluorescence measurements.

The production of sugar in the hydrolysis samples was measured to ensure that the substrate remained mainly unconverted during the experiment. Full conversion of 60 g/L Avicel would approximately make 185 mM cellobiose, and it follows from Figure 5 that the maximal conversion after 53 h

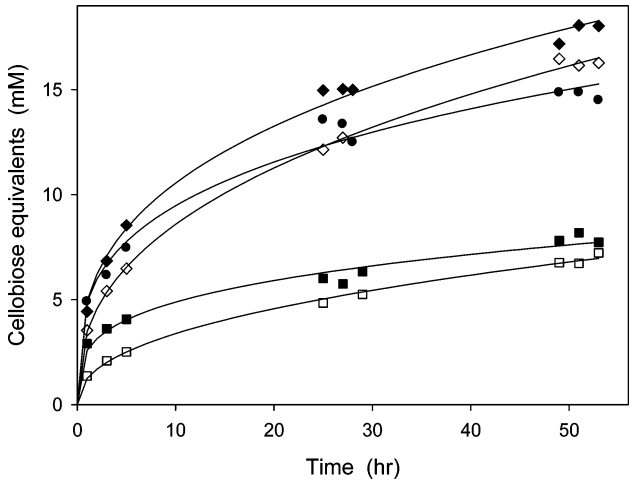

Figure 5. Concentration of soluble sugar in the samples analyzed by DSC. The product was predominantly cellobiose, but small amounts of glucose and cellotriose were also found. Results are given as cellobiose equivalents, i.e., $^1/_2$[glucose] + [cellobiose] + $^{11}/_2$[cellotriose]. Open symbols show data for Cel7A, and filled symbols are for Cel6A. The storage temperatures were 25 °C (squares), 40 °C (circles), and 49 °C (diamonds). The rate of the hydrolytic reaction was estimated from the slope of the fitted lines (sum of two exponentials).

was about 10%. The progress curves in Figure 5 were also used to assess the heat produced by the enzymatic reaction as this could potentially affect the DSC measurement. Thus, for the hydrolysis samples the enzyme was still catalytically active when the DSC measurement commenced; therefore, the thermal output necessarily reflected the sum of the heats from the thermal transition in the protein molecule (as seen in the reference samples) and a contribution from hydrolytic reaction. To assess the latter, we fitted an empirical function (a sum of two exponentials) to the progress curves and used the slope to estimate the hydrolytic rate. This analysis showed that for the first few time points the maximal slope in Figure 5 (for T_{store} = 49 °C) was about 1 mM/h. The hydrolytic heat flow (HF_{hyd} in units of J/s) is given as $HF_{hyd} = V_{cell}\Delta H_{hyd}v_{hyd}$, and the insertion of the enthalpy of Avicel hydrolysis $\Delta H_{hyd} \approx -4$ kJ/(mol cellobiose),[49] the volume of the calorimetric cell V_{cell} = 299 μL, and the rate $v_{hyd} \approx 1$ mM/h found above yields an expected HF_{hyd} of about 0.3 μW. This is negligible compared to the peak height in Figure 1, and even if HF_{hyd} increased 2- or 3-fold as the DSC temperature was raised from 49 °C (the temperature where HF_{hyd} was estimated) toward the maximal enzyme activity at around 60 °C,[43] it is still much smaller than the amplitude of the transition peaks in Figure 1 (20−35 μW). We therefore conclude that the contribution to the DSC signal arising from the hydrolysis reaction can be ignored in samples taken after 1 h. For samples taken at later stages the hydrolytic rate is lower (Figure 5) and HF_{hyd} will still be smaller. The absence of detectable effects from HF_{hyd} was also supported by the lack of a systematic upward curvature of the pretransition range of the DSC traces for hydrolysis samples. The small heat of reaction in the samples also rules out heating the Eppendorf tubes to temperatures above T_{store} in the incubator.

DISCUSSION

It is generally challenging to experimentally appraise the structure and stability of proteins adsorbed to solid surfaces. This relies on both practical limitations and difficulties in the interpretation of experimental observables with contributions from both protein and sorbent. For example, the suite spectroscopic methods that are commonly used in protein structure and stability studies are often limited by scattering, absorption, or competing signals from the solid material.[50] In a few cases, the stability of model proteins such as lysozyme, hemoglobin, or lactalbumin adsorbed on solid surfaces including silica and polystyrene has been assessed by DSC.[50−52] This experimental approach is nonspecific inasmuch as it detects the total heat flow arising from all processes during continuous heating. In the current context, this may provide the advantage of making it insensitive to the presence of the sorbent material as long as this material does not show any thermal transitions in the relevant temperature range. We found this criterion to be fulfilled for Avicel. Moreover, the heat produced by the enzymatic reaction was small enough not to disturb the detection of the transition in the enzyme, and we concluded that DSC can be applied to in situ stability studies of cellulases associated with (and actively hydrolyzing) a model substrate such as Avicel. Preliminary tests with (enzyme-free) lignocellulosic biomass in the DSC showed thermal transitions that could overlap with the denaturation of protein, thus suggesting that the method would be harder to apply for this substrate.

We first address the question of how to extract quantitative stability data from the calorimetric results. To this end we emphasize three general observations from the DSC measurements: (i) The transition temperature, T_T, was independent of the duration and storage temperature of the thermal stress experiment prior to the calorimetric measurement (Table 1 and Figure 2). (ii) The relative transition enthalpy, ΔH_{Rel}, decreased to different extents depending on the enzyme and the severity of the thermal stress experiment (Figure 3). (iii) Rescanning experiments suggested that all transitions in the DSC were irreversible, both for free and substrate-bound enzyme (no peak observed in the second scan). The simplest

dx.doi.org/10.1021/la500161e | Langmuir 2014, 30, 7134−7142

interpretation of these observations is that the native structure (free or substrate-bound) remained unchanged during thermal stress experiments (as T_T is constant), while the amount of native enzyme decreased to variable extents. This interpretation implies that the reduction in ΔH_{Rel} (Figure 3) reflects a gradual, irreversible loss of native enzyme during the experiment. In other words, some enzyme is already non-native before the DSC measurement and hence does not contribute to the transition peak (cf. Figures 1 and 5). This interpretation is along the lines of the so-called Lumry−Eyring (LE) model,[53] which is the most commonly applied description of irreversible protein denaturation. The LE model stipulates that a reversible change in the protein conformation precedes a kinetically controlled inactivation step, and this may be written as $E \overset{K}{\rightleftarrows} U \overset{k_i}{\rightarrow} I$, where E is the native enzyme, U is an unfolded (or partially unfolded) form, and I represents enzyme that has been irreversibly denatured through aggregation, misfolding, or covalent modifications.[54] Parameters K and k_i are, respectively, the equilibrium constant for the first step and the rate constant for the second. In the current context, this scheme pertains to the behavior of the reference samples, but an analogous denaturation process may be written for the substrate (S)-bound enzyme in the hydrolysis samples, $E'S \overset{K'}{\rightleftarrows} U'S \overset{k_i'}{\rightarrow} I'S$. These LE schemes underscore that two separate descriptors of stability must be distinguished. First, stability may be specified as the resistance toward irreversible inactivation by mild but prolonged thermal stress. This parameter is mainly governed by k_i (or k_i'), and we will henceforth call it long-term stability. (This is often called colloidal stability or kinetic stability in the literature,[55,56] but these terms are ambiguous when working with Avicel suspensions that are highly unstable from a colloidal point of view.) Second, stability may be defined as the resistance against conformational changes at higher temperatures, and we will call this intrinsic stability. For reversible transitions (i.e., when $k_i = 0$), the intrinsic stability is explicitly specified by the equilibrium constant K, and it can be derived rigorously from the measured transition temperature, T_T, and the enthalpy change. For irreversible transitions, such as those studied here, the interpretation of T_T is more complex. In particular T_T will depend on the scanning rate in a way that can be rationalized on the basis of the LE- picture.[57] We will not apply this detailed analysis here but will simply compare changes in T_T values obtained at the same scan rate and use these values as an operational measure of the intrinsic conformational stability, as is done in most DSC work on homogeneous systems. Samples from the thermal stress experiments were cooled to 20 °C in the DSC prior to the scan. The use of this low starting temperature was necessary in order to obtain a stabile baseline prior to the thermal transition and hence a precise determination of ΔH. Clearly, cooling from T_{store} to 20 °C could affect both enzyme binding and the E ⇄ U equilibrium, and it follows that the subsequent DSC heating scan will detect enzyme that is in dynamic equilibrium (i.e., in the E or U form) while the population captured in the I form will not be detected.

Intrinsic Stability. In the terminology specified above, the results in Table 1 show that the intrinsic stability of Cel7A was promoted by its association with substrate (T_T increased in the presence of substrate), while no significant change was found for Cel6A. The behavior of Cel7A parallels many earlier examples of increased intrinsic stability resulting from protein−ligand interactions in homogeneous solutions[48] but it is in contrast to DSC studies of the nonspecific adsorption of model proteins on solid surfaces, which showed pronounced reductions in T_T.[50,52] This probably reflects the specificity of the enzyme−substrate interaction and hence suggests that general properties of proteins on solid sorbents are of minor relevance in discussions of the stability of substrate-adsorbed cellulases. The absence of a measurable increase in the intrinsic stability of Cel6A upon association with substrate may rely on weaker interactions of this enzyme compared to those of Cel7A. This interpretation is in accord with both earlier work[34] and Figure 4, which shows a higher free enzyme concentration in the hydrolysis samples for Cel6A (implying weaker interactions of Cel6A compared to those of Cel7A). However, the behavior of T_T for Cel6A may also reflect a coupling between the two steps in the LE model. Thus, if the second (irreversible) step is fast (i.e., if k_i' is large), then the DSC signal will become asymmetric (as the U form is removed rapidly) and its maximum value (T_T) will be displaced toward lower temperatures.[57] Therefore, the unchanged value of T_T for Cel6A in Table 1 could reflect both weaker substrate interactions and a faster irreversible inactivation, which obscures the measurement of ΔT_T. The latter suggestion is in accord with both the lower long-term stability of Cel6A (see below) and the higher experimental scatter in T_T for Cel6A (Table 1), as dominance by the kinetically controlled step generally makes the thermograms more sensitive to technical subtleties.

Long-Term Stability. The long-term stability expressed as ΔH_{rel} depended on both the thermal stress and substrate interactions. The best long-term stability was found for Cel7A in buffer at T_{store} = 25 °C. Under these conditions ΔH_{rel} was unchanged for 53 h (Figure 4), and we conclude that the entire enzyme population remained in the native state (no accumulation of the I form in the sense of the LE scheme). Cel7A also showed good long-term stability at 25 °C in the hydrolysis samples. In this case, a linear fit to all ΔH_{Rel} data (Figure 4, left panel) showed a weak negative slope and a ΔH_{rel} value of around 0.97 after 53 h. This value is barely distinguishable from unity (ΔH_{rel} = 1 for a stable enzyme) within the experimental scatter (the slope of the fit was -5.5 ± 4 (SE) $\times 10^{-4}$ h^{-1}). At T_{stress} = 49 °C, ΔH_{Rel} for Cel7A fell to respectively 0.95 in the reference samples and 0.65 in the hydrolysis samples after 53 h. This implies that Cel7A has excellent physical stability in buffer at elevated temperatures but loses about a third of the native population when it is catalytically active. It is noticeable that the lower long-term stability of active enzyme occurred in spite of an increased intrinsic stability; in other words, the increased conformational stability that results from the interaction of Cel7A and its substrate (higher T_T in Table 1) does not translate into a better long-term stability. Free Cel6A showed approximately the same intrinsic stability as Cel7A, but Cel6A was far inferior with respect to long-term stability, in both reference and hydrolysis samples. At T_{store} = 49 °C, the ΔH_{Rel} data suggested that respectively 50% (reference) and 80% (hydrolysis) of the Cel6A population had been irreversibly denatured over the 53 h experiment. The analogous numbers at T_{store} = 40 °C were 35 and 50%. These results for Cel6A reiterate the conclusion for Cel7A that the long-term stability is much lower for active enzyme compared to enzyme in buffer. The above conclusions on long-term stability rest on the assumption that all enzyme in the hydrolysis samples was associated with the substrate. For Cel6A, however, a moderate fraction (about 15%, Figure 4) was

dx.doi.org/10.1021/la500161e | Langmuir 2014, 30, 7134−7142

in the aqueous phase. The influence of this on the DSC data can be assessed because the DSC behavior of free enzyme is known from the reference samples. Under the assumption that the DSC signal in the hydrolysis samples is a linear combination of contributions from free and bound enzyme, we found that the losses of native Cel6A at T_{store} = 40 and 49 °C were slightly larger than suggested in Figure 3, but the difference was comparable to the experimental scatter and hence was neglected. Molecular origins of the weaker interaction of Cel6A cannot be directly assessed on the basis of the current data. We speculate, however, that it could rely on the shorter and more open catalytic tunnel of Cel6A,[58] which is expected to contribute less to the net affinity than the longer and more closed tunnel of Cel7A.[59] This interpretation is supported by binding data for enzyme variants with no cellulose binding modules, which showed lower cellulose affinity for Cel6A than for Cel7A.[34] Finally, we note that in spite of a lower concentration of bound Cel6A (85%) compared to Cel7A (98%), the enzymatic activity of the former enzyme is comparable to or a bit higher than Cel7A (Figure 5). This is a sign of a slightly higher specific activity of Cel6A under the conditions studied here.

As described in the Introduction, one of the motivating factors of this work was the question of whether the long-term physical instability of the enzyme could be a cause of the slowdown in the hydrolytic rate. Some recent work has indeed supported this inference.[29] The data for Cel7A and T_{store} = 25 °C speak against any strict relationship because there is essentially no loss in the native population in the hydrolysis samples over the 53 h experiment (Figure 3). However, the hydrolytic rate, specified by the slope in Figure 5, fell by about 1 order of magnitude between 1 and 50 h of hydrolysis. This degree of slowdown is similar to what has previously been observed in a comparable experiment.[7] At higher storage temperatures, and particularly for Cel6A, the situation is quite different, and we found a conspicuous reduction in the native population in hydrolysis samples, particularly over the first 10 h (Figure 4). Taken together, these observations suggests that long-term instability cannot be the only cause of the slowdown but that it may become a significant factor under severe (industrially relevant) temperature conditions. At the higher storage temperatures, the importance of protein denaturation may be assessed by comparing the relative catalytic activity (e.g., the rate at a given time point divided by the initial rate; see Figure 5) and the relative enthalpy change, ΔH_{rel} (Figure 4). Attempts to do so showed that the relative activity always decreased more rapidly than ΔH_{rel}. If we consider the most unstable system studied (Cel6A at 49 °C) for t = 53 h, then ΔH was about 24% of the value after 1 h while the analogue fraction for the hydrolytic activity was only 8%. For the other (more stable) systems, this discrepancy was even larger, and this again shows that factors other than enzyme denaturation contribute significantly to the slowdown. For the current experiments, with final cellobiose concentrations in the 6−18 mM range, one such factor must be product inhibition.[8−10] It follows that future work combining DSC and more extensive activity measurements also including samples with added β-glucosidase (which converts cellobiose to the much less inhibitory glucose) could be useful in attempts to single out contributions to the slowdown. For the current purpose, we did not use β-glucosidase because the results would then have reflected combined effects of the long-term stability of both the cellobiohydrolase and the β-glucosidase.

We conclude that DSC is a promising tool for in situ measurements of both the intrinsic and long-term stability of cellulases actively associated with insoluble cellulose. Information of this type appears to be important to the understanding of cellulase kinetics, and we are not aware of other experimental approaches which have successfully monitored cellulase stability in situ. It is possible that methods including CD and fluorescence spectroscopy could be developed to provide direct information on structural changes in adsorbed cellulases, and this would be most valuable. However, earlier work has shown that it is difficult to filter out effects originating from the solid material in the spectroscopic data.[50] Another potential of the current method lies in its combined use with surface analysis methods such as QCM and SPR. These latter approaches have proven to be effective in characterizing the adsorption and activity of cellulases,[26−29] and a combination of this and data on the gradual loss of native structure (which cannot be detected by QCM or SPR) appears to be promising in attempts to reveal causes of the slowdown. The current results showed that the intrinsic stability of an adsorbed cellulase is readily measured but is a poor descriptor of long-term stability. Thus, Cel6A and Cel7A have comparable intrinsic stabilities, but Cel6A is much less stable in prolonged hydrolysis trials. We found that substrate association lead to increased (Cel7A) or unchanged (Cel6A) intrinsic stability and that substrate-associated (active) enzyme was less long-term stable than enzyme in pure buffer. This was particularly evident at T_{store} = 49 °C for Cel7A, which was fully stable in buffer but lost one-third of the native population during 53 h of hydrolysis. This suggests that shelf life tests including so-called "accelerated stability testing",[60] which are typically used to probe the robustness of industrial proteins, will tend to overestimate the stability of these cellulases. These conclusions were based on experiments with a pure cellulose substrate (Avicel), and no direct inference can be made with respect to the in situ stability of cellulases on lignocellulosic biomass. We suggest, however, that the effects seen here are the result of enzyme−cellulose interactions, which may also be relevant to more complex substrates, although other routes of inactivation may obviously be relevant or even dominant in biomass.

AUTHOR INFORMATION

Notes

The authors declare the following competing financial interest: Novozymes is a major enzyme-producing company.

ACKNOWLEDGMENTS

This work was supported by the Danish Council for Strategic Research, Program Commission on Sustainable Energy and Environment (grant nos. 2104-07-0028 and 11-116772 to P.W.)

REFERENCES

(1) Himmel, M. E.; Ding, S. Y.; Johnson, D. K.; Adney, W. S.; Nimlos, M. R.; Brady, J. W.; Foust, T. D. Biomass recalcitrance: Engineering plants and enzymes for biofuels production. *Science* **2007**, *315*, 804−807.

(2) Horn, S. J.; Vaaje-Kolstad, G.; Westereng, B.; Eijsink, V. G. H. Novel enzymes for the degradation of cellulose. *Biotechnol. Biofuels* **2012**, *5*.

(3) Kostylev, M.; Wilson, D. B. Synergistic interactions in cellulose hydrolysis. *Biofuels* **2012**, *3*, 61−70.

(4) Yang, B.; Dai, Z.; Ding, S.-Y.; Wyman, C. E. Enzymatic hydrolysis of cellulosic biomass. *Biofuels* **2011**, *2*, 421−450.
(5) Wilson, D. B. Cellulases and biofuels. *Curr. Opin. Biotechnol.* **2009**, *20*, 295−299.
(6) Bansal, P.; Hall, M.; Realff, M. J.; Lee, J. H.; Bommarius, A. S. Modeling cellulase kinetics on lignocellulosic substrates. *Biotechnol. Adv.* **2009**, *27*, 833−848.
(7) Bezerra, R. M. F.; Dias, A. A.; Fraga, I.; Pereira, A. N. Cellulose Hydrolysis by Cellobiohydrolase Cel7A Shows Mixed Hyperbolic Product Inhibition. *Appl. Biochem. Biotechnol.* **2011**, *165*, 178−189.
(8) Gruno, M.; Valjamae, P.; Pettersson, G.; Johansson, G. Inhibition of the Trichoderma reesei cellulases by cellobiose is strongly dependent on the nature of the substrate. *Biotechnol. Bioeng.* **2004**, *86*, 503−511.
(9) Murphy, L.; Bohlin, C.; Baumann, M. J.; Olsen, S. N.; Sorensen, T. H.; Anderson, L.; Borch, K.; Westh, P. Product inhibition of five Hypocrea jecorina cellulases. *Enzyme. Microb. Technol.* **2013**, *52*, 163−169.
(10) Teugjas, H.; Valjamae, P. Product inhibition of cellulases studied with 14C-labeled cellulose substrates. *Biotechnol. Biofuels* **2013**, *6*, 104.
(11) Zhang, S.; Wolfgang, D. E.; Wilson, D. B. Substrate heterogeneity causes the nonlinear kinetics of insoluble cellulose hydrolysis. *Biotechnol. Bioeng.* **1999**, *66*, 35−41.
(12) Murphy, L.; Cruys-Bagger, N.; Damgaard, H. D.; Baumann, M. J.; Olsen, S. N.; Borch, K.; Lassen, S. F.; Sweeney, M.; Tatsumi, H.; Westh, P. Origin of Initial Burst in Activity for Trichoderma reesei endo-Glucanases Hydrolyzing Insoluble Cellulose. *J. Biol. Chem.* **2012**, *287*, 1252−1260.
(13) Cruys-Bagger, N.; Elmerdahl, J.; Praestgaard, E.; Tatsumi, H.; Spodsberg, N.; Borch, K.; Westh, P. Pre-steady state kinetics for the hydrolysis of insoluble cellulose by Trichoderma reesei Cel7A. *J. Biol. Chem.* **2012**, *287*, 18451−18458.
(14) Jalak, J.; Kurashin, H.; Teugjas, H.; Valjamae, P. Endo-exo synergism in cllulase hydrolysis revisited. *J. Biol. Chem.* **2012**, *287*, 28802−28815.
(15) Jalak, J.; Valjamae, P. Mechanism of Initial Rapid Rate Retardation in Cellobiohydrolase Catalyzed Cellulose Hydrolysis. *Biotechnol. Bioeng.* **2010**, *106*, 871−883.
(16) Kurasin, M.; Valjamae, P. Processivity of Cellobiohydrolases Is Limited by the Substrate. *J. Biol. Chem.* **2011**, *286*, 169−177.
(17) Kipper, K.; Valjamae, P.; Johansson, G. Processive action of cellobiohydrolase Cel7A from Trichoderma reesei is revealed as 'burst' kinetics on fluorescent polymeric model substrates. *Biochem. J.* **2005**, *385*, 527−535.
(18) Praestgaard, E.; Elmerdahl, J.; Murphy, L.; Nymand, S.; McFarland, K. C.; Borch, K.; Westh, P. A kinetic model for the burst phase of processive cellulases. *FEBS J.* **2011**, *278*, 1547−1560.
(19) Harkins, T. T.; Lindsley, J. E. Pre-steady-state analysis of ATP hydrolysis by Saccharomyces cerevisiae DNA topoisomerase II. 1. A DNA-dependent burst in ATP hydrolysis. *Biochemistry* **1998**, *37*, 7292−7298.
(20) KnightC. G.Active-site titration of peptidases. In *Proteolytic Enzymes: Aspartic and Metallo Peptidases*; Barrett, A. J., Ed.; Academic Press: San Diego, 1995; Vol. *248*, pp 85−101.
(21) Takahashi, K.; Weiner, H. Nicotinamide adenine-dinucleotide activation of the esterase reaction of horse liver aldehyde dehydrogenase. *Biochemistry* **1981**, *20*, 2720−2726.
(22) Howell, J. A.; Mangat, M. Enzyme deactivation during cellulose hydrolysis. *Biotechnol. Bioeng.* **1978**, *20*, 847−863.
(23) Monschein, M.; Reisinger, C.; Nidetzky, B. Enzymatic hydrolysis of microcrystalline cellulose and pretreated wheat straw: A detailed comparison using convenient kinetic analysis. *Bioresour. Technol.* **2013**, *128*, 679−687.
(24) Olsen, S. N.; Lumby, E.; McFarland, K.; Borch, K.; Westh, P. Kinetics of Enzymatic High-Solid Hydrolysis of Lignocellulosic Biomass Studied by Calorimetry. *Appl. Biochem. Biotechnol.* **2011**, *163*, 626−635.
(25) Bubner, P.; Plank, H.; Nidetzky, B. Visualizing cellulase activity. *Biotechnol. Bioeng.* **2013**, *110*, 1529−1549.
(26) Cheng, G.; Liu, Z. L.; Murton, J. K.; Jablin, M.; Dubey, M.; Majewski, J.; Halbert, C.; Browning, J.; Ankner, J.; Akgun, B.; Wang, C.; Esker, A. R.; Sale, K. L.; Simmons, B. A.; Kent, M. S. Neutron Reflectometry and QCM-D Study of the Interaction of Cellulases with Films of Amorphous Cellulose. *Biomacromolecules* **2011**, *12*, 2216−2224.
(27) Maurer, S. A.; Bedbrook, C. N.; Radke, C. J. Competitive Sorption Kinetics of Inhibited Endo- and Exoglucanases on a Model Cellulose Substrate. *Langmuir* **2012**, *28*, 14598−14608.
(28) Turon, X.; Rojas, O. J.; Deinhammer, R. S. Enzymatic kinetics of cellulose hydrolysis: A QCM-D study. *Langmuir* **2008**, *24*, 3880−3887.
(29) Ma, A. Z.; Hu, Q.; Qu, Y. B.; Bai, Z. H.; Liu, W. F.; Zhuang, G. Q. The enzymatic hydrolysis rate of cellulose decreases with irreversible adsorption of cellobiohydrolase I. *Enzyme. Microb. Technol.* **2008**, *42*, 543−547.
(30) Kyriacou, A.; Neufeld, R. J.; Mackenzie, C. R. Reversibility and competition in the adsorption of trichoderma-reesei cellulase components. *Biotechnol. Bioeng.* **1989**, *33*, 631−637.
(31) Beldman, G.; Voragen, A. G. J.; Rombouts, F. M.; Searlevanleeuwen, M. F.; Pilnik, W. Adsorption and Kinetic-Behavior of Purified Endoglucanases and Exoglucanases from Trichoderma-Viride. *Biotechnol. Bioeng.* **1987**, *30*, 251−257.
(32) Nidetzky, B.; Steiner, W.; Claeyssens, M. Cellulose hydrolysis by cellulases from Trihoderma reesei: adsorptions of two cellobiohydrolases, two endocellulases and their core protein on filterpaper, and their relation to hydrolysis. *Biochem. J.* **1994**, *303*, 817−823.
(33) Bothwell, M. K.; Wilson, D. B.; Irwin, D. C.; Walker, L. P. Binding reversibility and surface exchange of Thermomonospora fusca E-3 and E-5 and Trichoderma reesei CBHI. *Enzyme. Microb. Technol.* **1997**, *20*, 411−417.
(34) Palonen, H.; Tenkanen, M.; Linder, M. Dynamic interaction of Trichoderma reesei cellobiohydrolases Cel6A and Cel7A and cellulose at equilibrium and during hydrolysis. *Appl. Environ. Microbiol.* **1999**, *65*, 5229−5233.
(35) Bentaleb, A.; Abele, A.; Haikel, Y.; Schaaf, P.; Voegel, J. C. FTIR-ATR and radiolabeling study of the adsorption of ribonuclease A onto hydrophilic surfaces: Correlation between the exchange rate and the interfacial denaturation. *Langmuir* **1998**, *14*, 6493−6500.
(36) Norde, W. Adsorption of proteins from solution at the solid-liquid interface. *Adv. Colloid Interface Sci.* **1986**, *25*, 267−340.
(37) Norde, W.; Anusiem, A. C. I. Adsorption, desorption and readsorption of proteins on solid-surfaces. *Colloids Surf.* **1992**, *66*, 73−80.
(38) Wertz, C. F.; Santore, M. M. Effect of surface hydrophobicity on adsorption and relaxation kinetics of albumin and fibrinogen: Single-species and competitive behavior. *Langmuir* **2001**, *17*, 3006−3016.
(39) Teeri, T. T. Crystalline cellulose degradation: New insight into the function of cellobiohydrolases. *Trends Biotechnol.* **1997**, *15*, 160−167.
(40) Ganner, T.; Bubner, P.; Eibinger, M.; Mayrhofer, C.; Plank, H.; Nidetzky, B. Dissecting and Reconstructing Synergism in situ visualization of cooperativity among cellulases. *J. Biol. Chem.* **2012**, *287*, 43215−43222.
(41) Hall, M.; Bansal, P.; Lee, J. H.; Realff, M. J.; Bommarius, A. S. Cellulose crystallinity - a key predictor of the enzymatic hydrolysis rate. *FEBS J.* **2010**, *277*, 1571−1582.
(42) Park, S.; Baker, J. O.; Himmel, M. E.; Parilla, P. A.; Johnson, D. K. Cellulose crystallinity index: measurement techniques and their impact on interpreting cellulase performance. *Biotechnol. Biofuels* **2010**, *3*, 10.
(43) Boer, H.; Koivula, A. The relationship between thermal stability and pH optimum studied with wild-type and mutant Trichoderma reesei cellobiohydrolase Cel7A. *Eur. J. Biochem.* **2003**, *270*, 841−848.
(44) Wu, I.; Arnold, F. H. Engineered thermostable fungal Cel6A and Cel7A cellobiohydrolases hydrolyze cellulose efficiently at elevated temperatures. *Biotechnol. Bioeng.* **2013**, *110*, 1874−1883.

(45) Baumann, M. J.; Borch, K.; Westh, P. Xylan oligosaccharides and cellobiohydrolase I (TrCel7A) interaction and effect on activity. *Biotechnol. Biofuels* **2011**, *4*, 45.
(46) Murphy, L.; Baumann, M. J.; Borch, K.; Sweeney, M.; Westh, P. An enzymatic signal amplification system for calorimetric studies of cellobiohydrolases. *Anal. Biochem.* **2010**, *404*, 140−148.
(47) Gasteiger, E.; Gattiker, A.; Hoogland, C.; Ivanyi, I.; Appel, R. D.; Bairoch, A. ExPASy: the proteomics server for in-depth protein knowledge and analysis. *Nucleic Acids Res.* **2003**, *31*, 3784−3788.
(48) Jelesarov, I.; Bosshard, H. R. Isothermal titration calorimetry and differential scanning calorimetry as complementary tools to investigate the energetics of biomolecular recognition. *J. Mol. Recognit.* **1999**, *12*, 3−18.
(49) Murphy, L.; Borch, K.; McFarland, K. C.; Bohlin, C.; Westh, P. A calorimetric assay for enzymatic saccharification of biomass. *Enzyme. Microb. Technol.* **2010**, *46*, 141−146.
(50) Haynes, C. A.; Norde, W. Structures and stabilities of adsorbed proteins. *J. Colloid Interface Sci.* **1995**, *169*, 313−328.
(51) Kleijn, M.; Norde, W. The adsorption of proteins from aqueous solution on solid surfaces. *Heterogen. Chem. Rev.* **1995**, *2*, 157−172.
(52) Steadman, B. L.; Thompson, K. C.; Middaugh, C. R.; Matsuno, K.; Vrona, S.; Lawson, E. Q.; Lewis, R. V. The effects of surface-adsorption on the thermal-stability of proteins. *Biotechnol. Bioeng.* **1992**, *40*, 8−15.
(53) Lumry, R.; Eyring, H. Conformation changes of proteins. *J. Phys. Chem.* **1954**, *58*, 110−120.
(54) Chi, E. Y.; Krishnan, S.; Randolph, T. W.; Carpenter, J. F. Physical stability of proteins in aqueous solution: Mechanism and driving forces in nonnative protein aggregation. *Pharm. Res.* **2003**, *20*, 1325−1336.
(55) Chi, E. Y.; Krishnan, S.; Kendrick, B. S.; Chang, B. S.; Carpenter, J. F.; Randolph, T. W. Roles of conformational stability and colloidal stability in the aggregation of recombinant human granulocyte colony-stimulating factor. *Protein Sci.* **2003**, *12*, 903−913.
(56) Sanchez-Ruiz, J. M. Protein kinetic stability. *Biophys. Chem.* **2010**, *148*, 1−15.
(57) Sanchezruiz, J. M. Theoretical-analysis of lumry-eyring models in differential scanning calorimetry. *Biophys. J.* **1992**, *61*, 921−935.
(58) Koivula, A.; Ruohonen, L.; Wohlfahrt, G.; Reinikainen, T.; Teeri, T. T.; Piens, K.; Claeyssens, M.; Weber, M.; Vasella, A.; Becker, D.; Sinnott, M. L.; Zou, J. Y.; Kleywegt, G. J.; Szardenings, M.; Stahlberg, J.; Jones, T. A. The active site of cellobiohydrolase Cel6A from Trichoderma reesei: The roles of aspartic acids D221 and D175. *J. Am. Chem. Soc.* **2002**, *124*, 10015−10024.
(59) Divne, C.; Stahlberg, J.; Teeri, T. T.; Jones, T. A. High-resolution crystal structures reveal how a cellulose chain is bound in the 50 angstrom long tunnel of cellobiohydrolase I from Trichoderma reesei. *J. Mol. Biol.* **1998**, *275*, 309−325.
(60) Franks, F. Accelerated stability testing of bioproducts - attractions and pitfalls. *Trends Biotechnol.* **1994**, *12*, 114−117.